Available online at www.sciencedirect.com
ScienceDirect
Acta Materialia 56 (2008) 1642–1649
Acta MATERIALIA
www.elsevier.com/locate/actamat

Homogeneous nucleation of dislocation loops in nanocrystalline metals and ceramics

M.Yu. Gutkin *, I.A. Ovid'ko

Institute of Problems of Mechanical Engineering, Russian Academy of Sciences, Bolshoj 61, Vasilievskii Ostrov, St. Petersburg 199178, Russia

Received 15 June 2007; received in revised form 2 December 2007; accepted 2 December 2007
Available online 6 February 2008

Abstract

A special mechanism of dislocation nucleation in deformed nanocrystalline metals and ceramics is theoretically described. The mechanism represents non-local homogeneous nucleation of a nanoscale loop of "non-crystallographic" partial dislocation whose Burgers vector magnitude continuously grows during the nucleation process. The dislocation loop nucleation is accompanied by nucleation and evolution of a generalized stacking fault bounded by the loop. It is shown that the special mechanism can effectively produce nanoscale loops of lattice dislocations in nanocrystalline metals (Al, Ni) and ceramics (3C–SiC) deformed at high mechanical stresses achieved in shock-wave and indentation load regimes.

Keywords: Nanocrystalline materials; Dislocations; Mechanical properties; Plastic deformation

1. Introduction

Nanocrystalline metals and ceramics show outstanding mechanical properties and are the subject of rapidly growing research efforts; see, for example, Refs. [1–34]. Superior strength and other unusual mechanical characteristics of nanocrystalline materials (NCMs) are associated with the specific action of lattice dislocation slip and interface-conducted deformation mechanisms in these materials [1–6,33,34]. In particular, standard dislocation sources, such as Frank–Read ones, are not effective in the generation of lattice dislocations in NCMs with the finest grains due to both nanoscale and interface effects [3,13]. This has led to interest in the identification and description of alternative sources of lattice dislocations in deformed NCMs. Following experimental data [17–22], computer simulations [23–29] and theoretical models [30,31], grain boundaries can effectively emit partial and perfect lattice dislocations during plastic deformation of NCMs. In doing so, lattice dislocations are seen to be generated by a heterogeneous nucleation mechanism at either pre-existing or intergrain-sliding-produced grain boundary dislocations. Recently, a special mechanism for homogeneous dislocation nucleation in grain interiors and boundaries of deformed NCMs has been suggested [35]. This mechanism represents the non-local homogeneous nucleation of a nanoscale loop of "non-crystallographic" partial dislocation whose Burgers vector magnitude, s, continuously grows during the nucleation process. In a first approximation examination under several simplifying assumptions [35], it was found that the non-local homogeneous nucleation can effectively produce perfect and partial dislocation loops in nanocrystalline Ni. The main aim of this paper is to theoretically describe in detail (without several simplifications assumed in Ref. [35]) the special mechanism for homogeneous dislocation nucleation in grain interiors of deformed NCMs. We will reveal analytical formulas for energy characteristics of the special mechanism of homogeneous dislocation nucleation. With these formulas, we will estimate the ranges of parameters (external stress level, dislocation loop size) within which the homogeneous nucleation of perfect and partial

* Corresponding author.
E-mail address: gutkin@def.ipme.ru (M.Yu. Gutkin).

1359-6454/$34.00 © 2007 Acta Materialia Inc. Published by Elsevier Ltd. All rights reserved.
doi:10.1016/j.actamat.2007.12.004

dislocation loops in nanoscale grain interiors is energetically favorable and occurs in a barrier-less way in typical nanocrystalline metals (Al, Ni) and ceramics (3C–SiC).

2. Basic features of the special mechanism for homogeneous nucleation of lattice dislocation loops in nanocrystalline metals and ceramics

Let us discuss the differences between the standard (see Figs. 1a–d and 2a–d) and the special mechanisms (see Figs. 1a, e–h and 2a, e–g) for homogeneous nucleation of lattice dislocations in NCMs. The standard mechanism for homogeneous nucleation of lattice dislocations in perfect crystals is realized through the local nucleation of a loop of either perfect or partial dislocation with a Burgers vector of constant magnitude, and its further expansion. Fig. 1a–d presents a three-dimensional (3D) illustration of the nucleation process in the case of a perfect dislocation loop with the Burgers vector, $\boldsymbol{B}$. Fig. 2a–d shows a two-dimensional (2D) view of the corresponding transformations of a model simple cubic crystalline lattice in a section (a plane that intersects the dislocation loop plane and is perpendicular to it) of the dislocation loop nucleated by the standard mechanism. The specific features of the standard mechanism for homogeneous nucleation of lattice dislocation loops are locality of its initial stage (the loop size starts to grow from 0) and constancy of magnitude of the Burgers vector during the loop generation process. This mechanism is characterized by a high energy barrier [36,37] and thereby hardly operates in real solids.

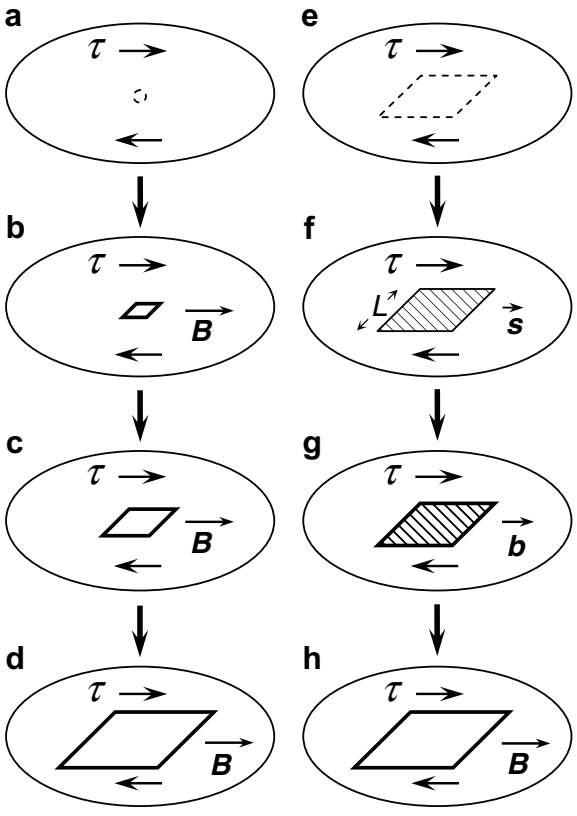

Fig. 1. Schematic three-dimensional representation of (a–d) standard homogeneous generation and extension of a gliding square loop of perfect lattice dislocation with Burgers vector $\boldsymbol{B}$ and (e)–(h) non-local homogeneous generation of a gliding square loop of "non-crystallographic" partial dislocation with a finite size L and small Burgers vector $\boldsymbol{s}$ ($0 < s \leqslant B$) under an external shear stress, τ. When s increases and achieves the magnitude b, the latter loop is transformed into a "normal" loop of partial lattice dislocation with Burgers vector $\boldsymbol{b}$; with further increase of s, it transforms into a "normal" loop of perfect lattice dislocation with Burgers vector $\boldsymbol{B} \approx 2\boldsymbol{b}$.

Following Ref. [35], we think that there exists an alternative mechanism for dislocation loop nucleation that can operate in NCMs deformed at high mechanical stresses. This mechanism is the non-local homogeneous nucleation of a "non-crystallographic" partial dislocation loop characterized by the Burgers vector magnitude, s, growing from zero to the Burgers vector magnitude of a partial lattice dislocation (b) and further to that of a perfect lattice dislocation ($B \approx 2b$). Let us discuss details of the special mechanism for dislocation loop nucleation in a mechanically loaded NCM; see a general 3D view in Fig. 1a and e–g and a 2D view in Fig. 2a and e–h, that illustrate the corresponding transformations of crystal lattice in a section (a plane that intersects the dislocation loop plane and is perpendicular to it) of the dislocation loop nucleated by the special mechanism. At the initial stage of the dislocation loop nucleation process, an applied shear stress causes a "momentary" ideal (rigid-body) shear to occur along the nanoscale rectangular plane fragment of crystal lattice in a grain (Figs. 1e and f and 2e). Such a shear is characterized by a small shear magnitude, s, and produces a generalized stacking fault that has sizes in the range from several to tens of nanometers (Figs. 1f and 2e). (In the theory of crystals, a generalized stacking fault is defined as a planar defect resulting from a cut of a perfect crystal across a single plane into two parts which are then subjected to a relative displacement through an arbitrary vector, **s** (lying in the cut plane) and rejoined; see, for example, Refs. [38–43].) The generalized stacking fault is bounded by the loop of a "non-crystallographic" partial dislocation characterized by a non-quantized ("non-crystallographic") Burgers vector, $\boldsymbol{s}$, with quite a small magnitude $s \ll b$ (Figs. 1f and 2e). At the following stage, the magnitude s of the dislocation Burgers vector continuously increases until it reaches the magnitude b of the Burgers vector of a partial lattice dislocation (Figs. 1g and 2f). Then s continuously grows further and finally reaches the magnitude B of the Burgers vector of a perfect lattice dislocation (Figs. 1h and 2g). The dislocation loop size, L, may increase during the nucleation process. The final state (Figs. 1h and 2g) resulting from the new mechanism is identical to that for the perfect lattice dislocation loop nucleated by the standard mechanism (Figs. 1d and 2d). The difference between the mechanisms can not be identified by conventional "post-mortem" experiments.

Thus, the specific features of the special mechanism for homogeneous nucleation of lattice dislocation loops are

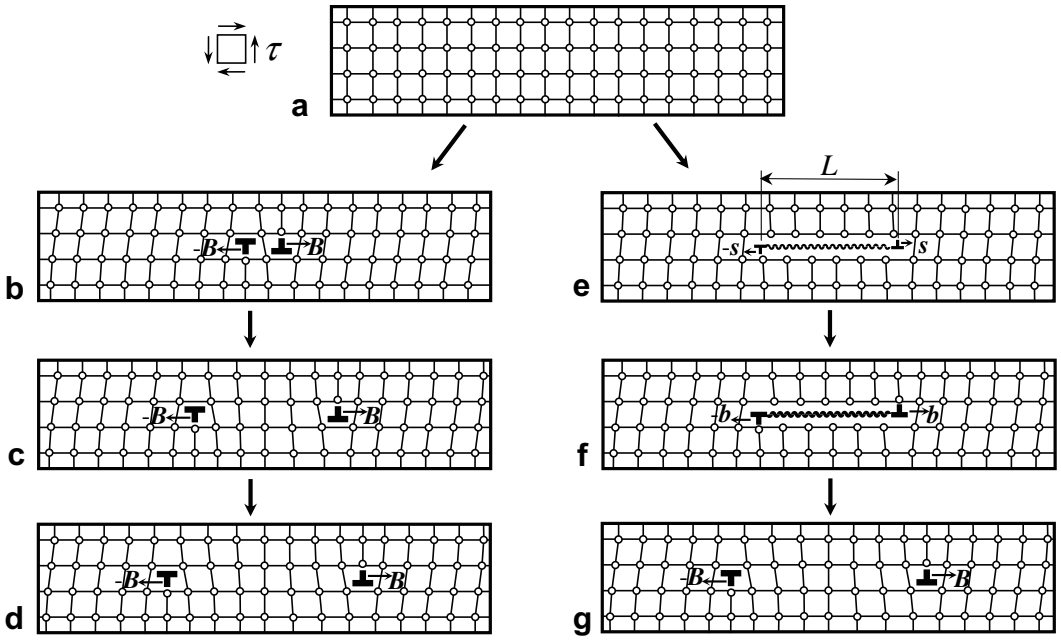

Fig. 2. Two-dimensional representation of crystal lattice transformations corresponding to (a–d) standard homogeneous generation and extension of a gliding square loop of perfect lattice dislocation with Burgers vector $\boldsymbol{B}$ and (e)–(g) non-local homogeneous generation of a gliding square loop of "non-crystallographic" partial dislocation with a finite size L and small Burgers vector $\boldsymbol{s}$ ($0 < s \leqslant B$) under an external shear stress, τ. When s increases and achieves the magnitude b, the latter loop is transformed into a "normal" loop of partial lattice dislocation with Burgers vector $\boldsymbol{b}$; with further increase of s, it transforms into a "normal" loop of perfect lattice dislocation with Burgers vector $\boldsymbol{B} \approx 2\boldsymbol{b}$.

non-locality of its initial stage (the loop size starts to grow from a finite value being in the range from several to tens of nanometers) and variability of Burgers vector magnitude during the loop generation process. (A similar process is also possible for the non-local homogeneous generation of a grain boundary dislocation loop [35]. Its detailed analysis is beyond the scope of this paper focused on dislocation loops in nanoscale grain interiors in NCMs.)

3. Energy characteristics of the special mechanism for homogeneous nucleation of lattice dislocation loops in nanocrystalline metals and ceramics

Let us consider energy characteristics for the homogeneous nucleation of a glide loop of "non-crystallographic" partial dislocation (Fig. 1a and e–h) in an infinite elastically isotropic solid under the action of an external shear stress, τ. Let the loop have the shape of a planar square of size L and be characterized by the Burgers vector $\boldsymbol{s}$, whose magnitude lies within the interval $0 < s \leqslant B$. When such a model dislocation loop is generated under the external shear stress τ, the total energy of the system is changed by the value ΔW:

$$\Delta W = W_e + W_\gamma - A \tag{1}$$

where W_e denotes the strain energy of the dislocation loop, W_γ the energy of the generalized stacking fault bounded by the loop and A the work spent by the shear stress τ to generate the loop.

In Ref. [35], the following simplifying assumptions were used in calculating the energy change, ΔW: the dislocation loop size, L, was assumed to be constant and the energy, γ, of the generalized stacking fault was assumed to be proportional to $\sin(\pi s/B)$, a simplest periodic function of s in the range from 0 to B. With these assumptions, the energy change, ΔW, was calculated and estimated in the case of nanocrystalline Ni [35]. In this paper, we suppose that the dislocation loop size, L, may change during the loop generation process and a more realistic "two-humped" dependence $\gamma(s)$ is used which is based on the corresponding computer simulations [39–43] of the energy of the generalized stacking faults in various solids. In the framework of this approach (avoiding the simplifications assumed in Ref. [35]), we will calculate and estimate the energy change, ΔW, characterizing the special mechanism for the generation of nanoscale loops of lattice dislocations in nanocrystalline metals (Al, Ni) and ceramics (3C–SiC).

Let us calculate the terms on the right-hand side of Eq. (1). In the case of a square loop of size L, W_e can be adapted from Ref. [44] as follows:

$$W_e \approx Ds^3(2-\nu)\frac{L}{s}\left(\ln\frac{L}{s} - 0.78\right) \tag{2}$$

where $D = G/[2\pi(1-\nu)]$, G is the shear modulus and ν is the Poisson ratio.

Let us consider the term W_γ that characterizes the energy of the generalized stacking fault. In general, with the definition of generalized stacking faults [38–43], W_γ varies with increasing Burgers vector magnitude, s. Recently, several research groups have reported on computer simulations of dependences of the specific (per unit area) energy γ on the shear, s, characterizing generalized

stacking faults in various solids; see, for example, [39–43] and references therein. These dependences typically represent "two-humped" curves. Each "two-humped" dependence has its minimum corresponding to the specific energy, γ_0, of a conventional stable stacking fault and two maxima corresponding to the energy, γ_m, of two unstable stacking faults. In our model, we use a "two-humped" dependence, $\gamma(s)$, approximated as follows:

$$\gamma(s)=\begin{cases}\gamma_m \sin\frac{2\pi s}{B}, & \text{if } s<\frac{B}{4}\\ \frac{\gamma_m+\gamma_0}{2}-\frac{\gamma_m-\gamma_0}{2}\cos\frac{4\pi s}{B}, & \text{if } \frac{B}{4}\leqslant s<\frac{3B}{4}\\ -\gamma_m \sin\frac{2\pi s}{B}, & \text{if } \frac{3B}{4}\leqslant s\leqslant B\end{cases} \quad (3)$$

In the situation under discussion, the generalized stacking fault energy, W_γ, is supposed to consist of two terms. The first term corresponds to the energy of the generalized stacking fault within the area $(L-2s)^2$, while the second term describes the energy of the fault just around the loop line. When the "non-crystallographic" dislocation loop is transformed into a loop of conventional partial dislocation ($s=b$), the first term achieves a value of γ_0, while the second term transforms into the energy of the core of the partial dislocation loop. As a result, W_γ reads:

$$W_\gamma=\gamma(s)(L-2s)^2+Ds^2 2L(2-\nu) \quad (4)$$

The work A spent by the shear stress τ to generate the dislocation loop is given by the following standard expression:

$$A=L^2 s\tau \quad (5)$$

With formulas (1)–(5), after some algebra, the energy change, ΔW, can be written as:

$$\Delta W=Db^3\left\{x^2 y(2-\nu)\left(\ln\frac{y}{x}+1.22\right)+(y-2x)^2\frac{\gamma(x)}{Db}-xy^2\frac{\tau}{D}\right\} \quad (6)$$

where $x=s/b$ and $y=L/b$ are the dimensionless parameters and $\gamma(x)$ is given by Eq. (3).

We calculated function $\Delta W(x,y)$ in the three exemplary cases of materials with face-centered cubic crystal lattices: aluminium (Al), nickel (Ni) and the cubic phase of silicon carbide (3C–SiC). In our calculations, the following values of the model parameters were used. With data from Ref. [36], for Al, we used $G=27$ GPa, $\nu=0.31$ and $b\approx 0.143$ nm. The minimum and maximum values of the specific energy of a generalized stacking fault, for Al, were approximated by the corresponding values resulted from tight-binding calculations [41]: $\gamma_0=99$ mJ m^{-2} and $\gamma_m=164$ mJ m^{-2}, respectively. The values of parameters for Ni were chosen as [36,42]: $G=73$ GPa, $\nu=0.34$, $b\approx 0.125$ nm, $\gamma_0\approx 120$ mJ m^{-2} and $\gamma_m\approx 170$ mJ m^{-2}. In the case of 3C–SiC, we used the following values of parameters [45,46]: $G=217$ GPa, $\nu=0.23$ and $b\approx 0.154$ nm. Also, for 3C–SiC, we took the value of the specific energy, γ_0, to be $\gamma_0\approx 0.1$ mJ m^{-2}, as measured in Ref. [47]. At the same time, we failed to find any experimental value or estimate of γ_m. In these circumstances, for 3C–SiC, we approximated γ_m by $k\gamma_0$ with values of $k=2$, 10 and 25. (Values of the ratio $k=\gamma_m/\gamma_0$ for covalent solids, such as 3C–SiC, are expected to be larger than those characterizing metals. This statement is supported by computer simulations [39] of the generalized stacking fault energy of silicon, a typical covalent solid, showing k to be around 10 or more.) Our calculations revealed that numerical estimates of the energy change, ΔW, for 3C–SiC, weakly depend on k, because γ_0 and γ_m are rather small in all the cases under examination.

With Eq. (1), we calculated the maps for the energy change function, $\Delta W(x,y)$. These maps are shown in Figs. 3–5, for Al, Ni and 3C–SiC (with $k=25$), respectively, at various magnitudes of the applied shear stress, τ.

For Al and Ni, the energy maps are similar in their general features. In both the cases, when τ is relatively small, there are two characteristic energy barriers along the axes $x=s/b$ and $y=L/b$ (Figs. 3a and b and 4a and b). These barriers must be overcome in order to nucleate a dislocation loop. For Al, the saddle points ΔW_s ($\tau=2$ GPa) $\approx$ 4.55 eV and ΔW_s ($\tau=3$ GPa) $\approx$ 1.11 eV have approximate coordinates (0.83, 22) and (0.62, 12), respectively, in the (s/b, L/b) space. For Ni, the saddle points ΔW_s ($\tau=3$ GPa) $\approx$ 19.05 eV and ΔW_s ($\tau=4$ GPa) $\approx$ 6.35 eV are located approximately at (0.72, 48) and (0.49, 36), respectively, in the (s/b, L/b) space. These values of ΔW_s are high and the loop hardly can nucleate.

If τ is large enough ($\tau\geqslant 3.7$ GPa for Al and $\tau\geqslant 4.4$ GPa for Ni), the situation drastically changes (see Figs. 3c and d and 4c and d). The "left" energy barriers disappear and a dislocation loop can nucleate through increase of its strength, s, and size, L, without any barrier. The thick arrowed curves approximately show the barrier-less evolution of a dislocation loop in the (s/b, L/b) space or, in other terms, the (x,y) space. Let us consider in detail the stages of barrier-less evolution shown in Figs. 3c and d and 4c and d. When τ is comparatively small, as illustrated in Figs. 3c and 4c, the dislocation loop first grows mainly in size. The dislocation strength, s, is rather low ($s\leqslant b/20$) at this stage. When the dislocation loop parameters, s and L, achieve the first critical region ($x\approx x_{c1}$, $y\approx y_{c1}$) in the map of $\Delta W(x,y)$, the loop stops extending and starts to grow in strength. The point (x_{c1},y_{c1}) corresponds to disappearance of "left" minima at the contours $y(x)$. As a result, the loop of fixed size increases in strength and finally transforms into a loop of perfect lattice dislocation. When τ is comparatively large, as illustrated in Figs. 3d and 4d, the loop first grows in both size and strength (here $s\leqslant b/10$) and also attains the first critical region. After this event, the dislocation loop increases in strength until $x\approx 1$, corresponding to the Burgers vector of a partial lattice dislocation. This area of the map may be considered as the second critical region ($x\approx x_{c2}$, $y\approx y_{c2}$), where the "right" minima at the contours $y(x)$ appear. Let us consider evolution of the dislocation loop parameters in the map area between the second critical region and the third critical region ($x\approx x_{c3}$, $y\approx y_{c3}$), where the "right" minima at the contours $y(x)$ disappear. Evolution of the dislocation loop

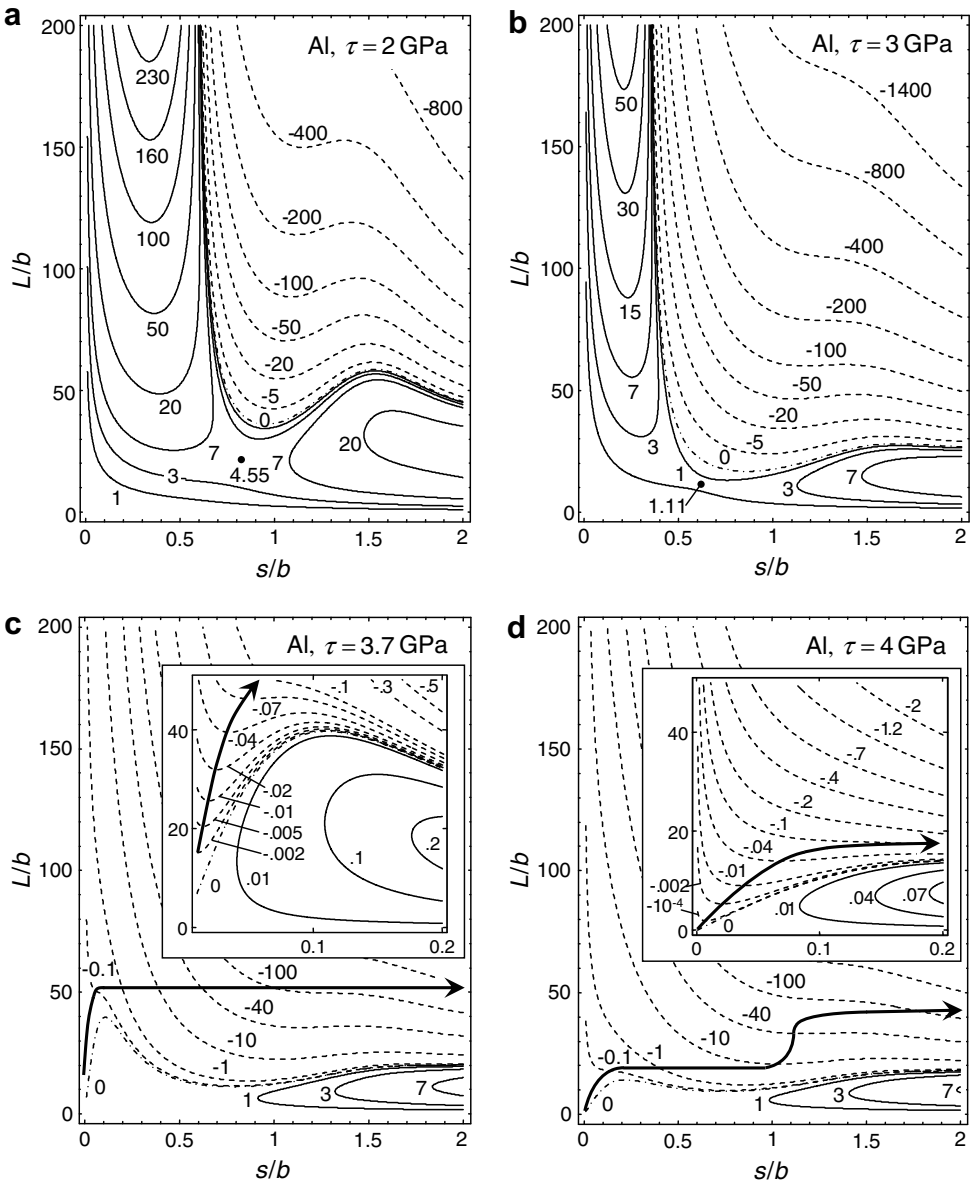

Fig. 3. Maps of the energy change $\Delta W(x,y)$, where $x = s/b$ and $y = L/b$, for pure Al under the external shear stress (a) $\tau = 2$ GPa, (b) 3 GPa, (c) 3.7 GPa and (d) 4 GPa. The values of ΔW are given in electron-volts. The bold dots in maps (a, b) show the saddle points. The thick arrowed curves in maps (c, d) approximately image the barrier-less evolution of a dislocation loop in strength and size. The insets in plots (c, d) show the enlarged maps for small s and L.

parameters in this map area occurs through growth of both the size and strength of the loop. When the loop parameters, s and L, cross the third critical region, the dislocation loop again practically stops extending and only increases in strength until it reaches the Burgers vector of perfect lattice dislocation.

Our calculations show that homogeneous nucleation of dislocation loops in Al and Ni is only possible under rather high stress levels. It is interesting to note that using both computer simulation and analytical analysis, de Koning et al. [48] discovered and described an intermediate (not purely homogeneous) mechanism of nucleation of partial dislocation loops. In their simulation of the Frank–Read source in pure Al, under some special orientations of the external shear stress with respect to the Burgers vector of the incipient dislocation segment, first, a loop of Shockley partial dislocation was generated at the incipient segment and, secondly, another loop of Shockley partial dislocation with different Burgers vector was nucleated quasi-homogeneously within the area of the intrinsic stacking fault inside the first dislocation loop. As a result, the combination of the first and second partial loops produced a loop of perfect dislocation with the Burgers vector different from that of the incipient dislocation segment (see Ref. [48] for more details). Of course, such a two-step generation process needs a signif-

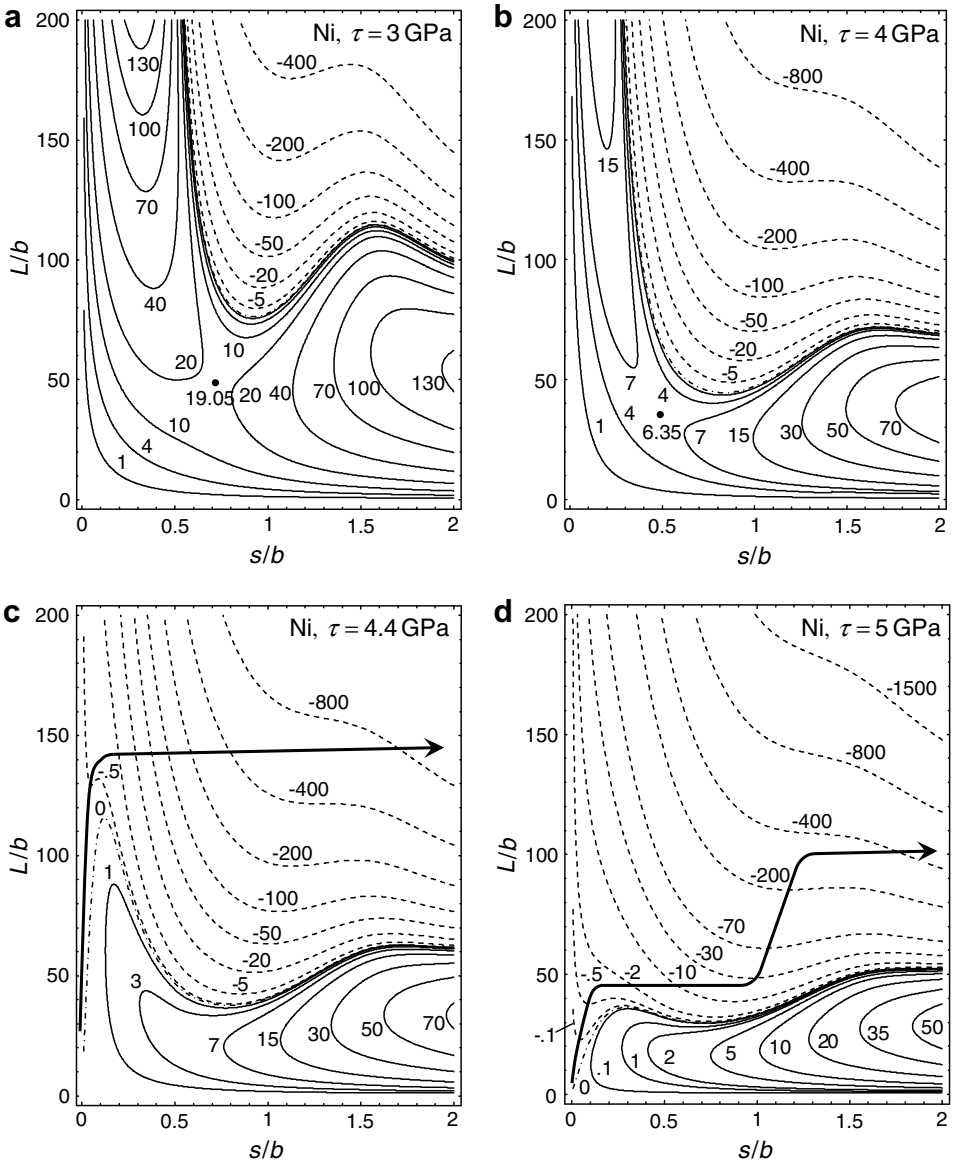

Fig. 4. Maps of the energy change $\Delta W(x,y)$, where $x = s/b$ and $y = L/b$, for pure Ni under the external shear stress (a) $\tau = 3$ GPa, (b) 4 GPa, (c) 4.4 GPa and (d) 5 GPa. The values of ΔW are given in electron-volts. The bold dots in maps (a, b) show the saddle points. The thick arrowed curves in maps (c, d) approximately image the barrier-less evolution of a dislocation loop in strength and size.

icantly lower level of external shear stress (≈1.2–1.7 GPa [48]), because the first step is purely heterogeneous nucleation of a partial loop at the Frank–Read source, while the second step is quasi-homogeneous nucleation of a partial loop within the pre-existing intrinsic stacking fault.

In the case of 3C–SiC, the characteristic maps of $\Delta W(x,y)$ are rather simple. The region of negative values of $\Delta W(x,y)$ becomes wider with rising τ. If τ is small (Fig. 5a), this region is rather narrow and a nucleating dislocation loop can grow in size without any significant increase in its strength. When τ becomes much higher (Fig. 5b and c), the loop grows in both size and strength. It is interesting to note that the curve, which images the barrier-less loop evolution, remains practically linear for all taken values of τ. We can conclude that, due to the very low values of stacking fault energies γ_0 and γ_m of 3C–SiC, dislocation loop nucleation by the special mechanism is energetically favorable even at rather low (for 3C–SiC) values of τ. In this context, the special mechanism is expected to play an important role in 3C–SiC ceramics with either nanocrystalline or coarse-grained structures, where the Peierls barrier is rather high and conventional dislocation slip is suppressed.

To summarize, a special mechanism for dislocation nucleation is energetically favorable and occurs in a barrier-less way in nanocrystalline metals (Al, Ni) and ceramics (3C–SiC) deformed at high mechanical stresses. This level of external stress is achievable, at least in shock-wave and indentation load regimes.

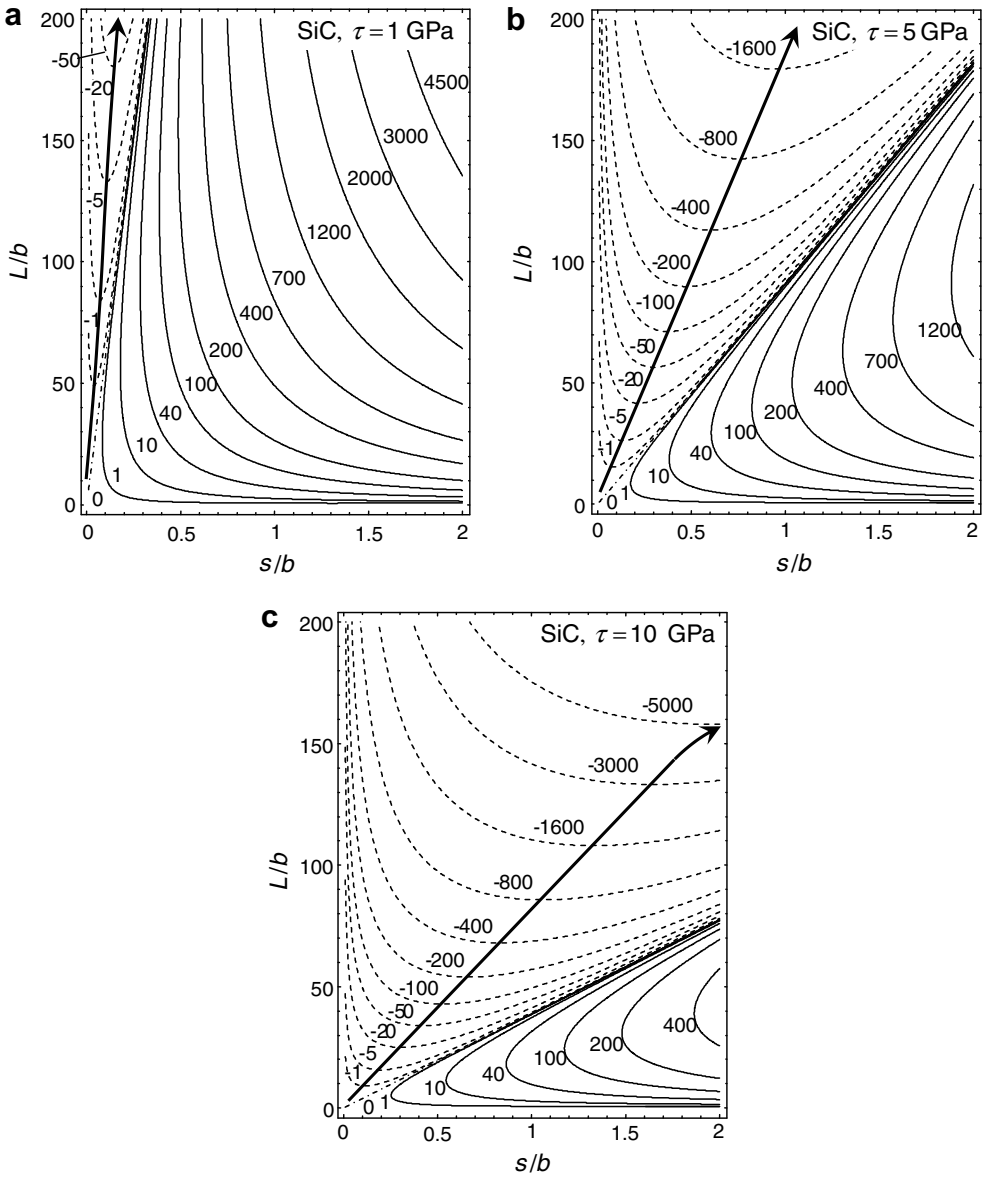

Fig. 5. Maps of the energy change $\Delta W(x,y)$, where $x = s/b$ and $y = L/b$, for 3C–SiC under the external shear stress (a) $\tau = 1$ GPa, (b) 5 GPa and (c) 10 GPa. The values of ΔW are given in electron-volts. The thick arrowed curves approximately image the barrier-less evolution of a dislocation loop in strength and size.

4. Concluding remarks

Thus, in this paper a special mechanism for dislocation nucleation in deformed NCMs – non-local homogeneous nucleation of "non-crystallographic" dislocation loops with continuously growing Burgers vector magnitude (Figs. 1e–h and 2e–h) – has been theoretically described. According to our analysis of the energy characteristics of the special mechanism, it can effectively operate in a barrier-less way and produce loops of partial and perfect lattice dislocations in nanocrystalline metals (Al, Ni) and ceramics (3C–SiC) deformed at high mechanical stresses. This level of external stress can be achieved in shock-wave and indentation load regimes. Besides, with the existence of numerous stress sources (such as dislocations and disclinations) and concentrators (such as pores and cracks) in NCMs [1–6, 33,34], local stresses can reach very high values and thereby cause homogeneous nucleation of dislocation loops in these materials even under quasistatic load regimes.

Recently, ultrahigh strain rates ($>10^7\ s^{-1}$) and pressures (20–70 GPa) have been achieved in experiments [49] on laser-driven compression of nanocrystalline Ni with grain sizes of 30–100 nm. Post-mortem transmission electron microscopy characterization revealed that the nanocrystalline structures survived the shock load and that dislocation slip mechanism is essential or even dominant. In particular, the dislocation density was estimated to be around $10^{16} m^{-2}$

in a nanocrystalline Ni sample after compression at 40 GPa pressure on nanosecond timescales. The origin of this remarkably high dislocation density has been not identified. In the context of the theoretical results presented in this paper, the non-local homogeneous nucleation of dislocation loops appears to be a strong candidate to be responsible for generation of high-density dislocation ensembles in nanocrystalline Ni (and, probably, other NCMs) under shock-wave deformation.

In general, the representations of the new dislocation nucleation mechanism (Figs. 1e–h and 2e–g) should be taken into account in future experimental and theoretical examinations of the dislocation activity in NCMs. Of special importance would be experimental "in situ" observation of the dislocation loop nucleation events in deformed NCMs with various compositions and geometric parameters. This has the potential to allow identification of the conditions under which the special dislocation nucleation mechanism is dominant. Finally, the special mechanism for dislocation nucleation is of great fundamental interest, because it can effectively contribute to relaxation processes in diverse solids such as conventional polycrystals, Gum Metal [50], nanocomposites [51] and nanoscale films [52]. In particular, the theoretical analysis given in this paper is directly applicable to a description of the special mechanism for dislocation nucleation in conventional polycrystals. With results of our theoretical analysis, the non-local homogeneous nucleation of nanoscale dislocation loops is energetically favorable in conventional polycrystals under shock-wave and indentation load regimes. However, standard dislocation sources, such as Frank–Read ones, are also effective in generation of lattice dislocations in conventional polycrystals even at low external stresses, in contrast to NCMs. Therefore, the role of the special mechanism in dislocation nucleation in conventional polycrystals is hardly essential.

Acknowledgements

The work was supported, in part, by the Russian Federal Agency of Science and Innovations (Contract 02.513.11.3190 of the Program "Industry of Nanosystems and Materials"), the National Science Foundation under Grant CMMI No. 0700272, the Russian Science Support Foundation, CRDF (Grant No. RUE2-2684-ST-05), the Russian Academy of Sciences Program "Structural Mechanics of Materials and Construction Elements" and St. Petersburg Center of Russian Academy of Sciences.

References

[1] Kumar KS, Suresh S, van Swygenhoven H. Acta Mater 2003;51:5743.
[2] Tjong SC, Chen H. Mater Sci Eng R 2004;45:1.
[3] Wolf D, Yamakov V, Phillpot SR, Mukherjee AK, Gleiter H. Acta Mater 2005;53:1.
[4] Han BQ, Lavernia E, Mohamed FA. Rev Adv Mater Sci 2005;9:1.
[5] Ovid'ko IA. Int Mater Rev 2005;50:65.
[6] Meyers MA, Mishra A, Benson DJ. Progr Mater Sci 2006;51:427.
[7] Fedorov AA, Gutkin MYu, Ovid'ko IA. Acta Mater 2003;51:887.
[8] Zhan G-D, Kuntz JD, Wan J, Mukherjee AK. Nature Mater 2003;2:38.
[9] Cheng S, Spencer JA, Milligan WW. Acta Mater 2003;51:4505.
[10] Xia Z, Riester L, Curtin WA, Li H, Sheldon BW, Liang J, et al. Acta Mater 2004;52:931.
[11] Gutkin MYu, Ovid'ko IA, Skiba NV. Acta Mater 2004;52:1711.
[12] Wang YM, Ma E. Acta Mater 2004;52:1699.
[13] Weissmueller J, Markmann J. Adv Eng Mater 2005;7:202.
[14] Cheng S, Ma E, Wang YM, Kecskes LJ, Youssef KM, Koch CC, et al. Acta Mater 2005;53:1521.
[15] Ovid'ko IA, Sheinerman AG. Acta Mater 2005;53:1347.
[16] Xu X, Nishimura T, Hirosaki N, Xie R-J, Yamamoto Y, Tanaka H. Acta Mater 2006;54:255.
[17] Mukherjee AK. Mater Sci Eng A 2002;322:1.
[18] Liao XZ, Zhou F, Lavernia EJ, He DW, Zhu YT. Appl Phys Lett 2003;83:5062.
[19] Chen MW, Ma E, Hemker KJ, Sheng HW, Wang YM, Cheng XM. Science 2003;300:1275.
[20] Kumar KS, Suresh S, Chisholm MF, Norton JA, Wang P. Acta Mater 2003;51:387.
[21] Liao XZ, Zhou F, Srinivasan SG, Zhu YT, Valiev RZ, Gunderov DV. Appl Phys Lett 2004;84:592.
[22] Wu XL, Qi Y, Zhu YT. Appl Phys Lett 2007;90:221911.
[23] Van Swygenhoven H, Spaczer M, Caro A. Acta Mater 1999;47:3117.
[24] Yamakov V, Wolf D, Salazar M, Phillpot SR, Gleiter H. Acta Mater 2001;49:2713.
[25] Frozeth AG, Derlet PM, Van Swygenhoven H. Acta Mater 2004;52:5863.
[26] Frozeth AG, Derlet PM, Van Swygenhoven H. Acta Mater 2004;52:2259.
[27] Hasnaoui A, Derlet PM, Van Swygenhoven H. Acta Mater 2004;52:2251.
[28] Schiotz J. Scr Mater 2004;51:837.
[29] Shimokawa T, Nakatani A, Kitagawa H. Phys Rev B 2005;71:224110.
[30] Bobylev SV, Gutkin MYu, Ovid'ko IA. Acta Mater 2004;52:3793.
[31] Bobylev SV, Gutkin MYu, Ovid'ko IA. Phys Rev B 2006;73:064102.
[32] Koch CC. J Mater Sci 2007;42:1403.
[33] Gutkin MYu, Ovid'ko IA. Plastic deformation in nanocrystalline materials. Berlin: Springer; 2004.
[34] Koch CC, Ovid'ko IA, Seal S, Veprek S. Structural nanocrystalline materials: fundamentals and applications. Cambridge: Cambridge University Press; 2007.
[35] Gutkin MYu, Ovid'ko IA. Appl Phys Lett 2006;88:211901.
[36] Hirth JP, Lothe J. Theory of dislocations. New York (NY): Wiley; 1982.
[37] Xu G, Argon AS. Phil Mag Lett 2000;80:605.
[38] Vitek V. Philos Mag 1968;18:773.
[39] Joos B, Ren Q, Duesbery MS. Phys Rev B 1994;50:5890.
[40] Lu G, Kioussis N, Bulatov VV, Kaxiras N. Phys Rev B 2000;62:3099.
[41] Bernstein N, Tadmor EB. Phys Rev B 2004;69:094116.
[42] Van Swygenhoven H, Derlet PM, Frøseth AG. Nat Mater 2004;3:399.
[43] Lazar P, Podloucky DC. Phys Rev B 2007;75:024112.
[44] Gutkin MYu, Sheinerman AG. Phys Stat Sol (b) 2004;241:1810.
[45] Lambrecht WRL, Segall B, Methfessel M, van Schilfgaarde M. Phys Rev B 1991;44:3685.
[46] Kräußlich J, Bauer A, Köcher B, Goetz K. Mater Sci Forum 2001;353–356:319.
[47] Kaiser U, Khodos II. Phil Mag A 2002;82:541.
[48] de Koning M, Cai W, Bulatov VV. Phys Rev Lett 2003;91:025503.
[49] Wang YM, Bringa EM, McNaney JM, Victoria M, Caro A, Hodge AM, et al. Appl Phys Lett 2006;88:061917.
[50] Gutkin MYu, Ishizaki T, Kuramoto S, Ovid'ko IA. Acta Mater 2006;54:2489.
[51] Ovid'ko IA, Sheinerman AG. J Phys Condens Matter 2006;18:L225.
[52] Ovid'ko IA, Sheinerman AG. J Phys Condens Matter 2007;19:056008.